AIMS Mathematics, 10(11): 26106–26131.
DOI: 10.3934/math.20251149
Received: 23 August 2025
Revised: 21 October 2025
Accepted: 29 October 2025
Published: 12 November 2025

https://www.aimspress.com/journal/Math

Research article

Change point estimation of hazard rates in contaminated Birnbaum-Saunders models with an application to tuberculosis survival data

Farouq Mohammad A. Alam*

Department of Statistics, Faculty of Science, King Abdulaziz University, Jeddah 21589, Saudi Arabia

* **Correspondence:** Email: fmalam@kau.edu.sa.

Abstract: In reliability and survival analysis, the hazard rate is a key statistical measure that quantifies the instantaneous risk of an event occurring at a given time. Detecting a change point in the hazard rate is particularly important in biomedical and reliability studies, as it may indicate a shift in the underlying failure mechanism or disease progression. This paper addresses the estimation of hazard rate change points under the contaminated Birnbaum-Saunders model, a positively skewed lifetime distribution originally derived from material fatigue theory but now widely applied in diverse fields. Several estimation methods were considered, and their performance was compared in terms of estimation efficiency and robustness when the data are subject to contamination. To assess finite-sample properties, extensive Monte Carlo simulations were carried out, highlighting the strengths and limitations of each estimator under varying contamination levels. In addition to the simulation study, the proposed methods were applied to a real biomedical dataset involving the survival times of guinea pigs (cavia corcellus) injected with different dosages of Mycobacterium tuberculosis, the pathogen that causes tuberculosis. The application demonstrates the practical value of the comparative results and provides insight into disease progression under varying infection intensities. Overall, the study contributes to the literature by offering both methodological evaluation and an applied perspective on change point estimation in hazard rates.

Keywords: point estimation; change point estimation; hazard rate; Birnbaum-Saunders distribution; survival data analysis
Mathematics Subject Classification: 62F10, 62N05

1. Introduction

Determining the change point of a hazard rate, that is, the peak point of the hazard function, is of practical importance in reliability and biomedical studies. By approximating such an instant of change, researchers can implement appropriate interventions for the phenomenon under study. For

instance, suppose that medical scientists begin administering a treatment for a specific disease. Once they identify the time at which the hazard rate starts to decline, they may reduce or discontinue the dosage, thereby lowering treatment costs while maintaining effectiveness. Relevant research articles include the following. The change point of the hazard function of the Birnbaum-Saunders (BS) distribution was discussed in [1]. They verified that the hazard function is unimodal for all values of the shape parameter; see also [2] in this regard. They further explained different approaches to obtain the change point, conducted assessments via Monte Carlo simulations, and analyzed data to illustrate their findings. In [3], the change point of the hazard function was studied in the case of the Student's t-BS distribution, a special case of the generalized BS distribution that also generalizes both the Cauchy BS distribution and the conventional BS distribution. They carried out numerical applications to evaluate the efficiency of the change point estimation using several methods and presented empirical results. More recently, [4] investigated the behavior of the hazard rate function of the logistic BS distribution and developed associated inference procedures.

To estimate the hazard rate or one of its characteristics (such as the change point), it is first necessary to estimate the underlying model parameters using an appropriate statistical method. The maximum likelihood framework is most commonly employed for this purpose. However, in the statistical literature, a variety of alternative estimation methods have been proposed, some of which may outperform the maximum likelihood estimator (MLE) under certain conditions, particularly in the presence of data contamination (i.e., outliers or extreme observations). As a result, numerous researchers have undertaken comparative studies to examine, through numerical investigations, the relative performance of different estimation approaches from various perspectives and circumstances; see, for example, [5–9], among other contributions cited in these studies. In practice, the efficiency of estimation is strongly influenced by the quality of the data. A dataset free from contamination (i.e., outliers or extreme observations) is always preferred, as it ensures the highest possible estimation efficiency. However, in most scientific studies, there is no guarantee that the collected data are uncontaminated. Frequentist estimation methods, such as maximum likelihood, are well known to lack robustness in the presence of outliers, since the distortions caused by such observations can substantially degrade the performance of estimators. A simple illustration is the comparison between the maximum likelihood estimator of the scale parameter in the exponential distribution and the nonparametric estimator of the same parameter based on the median, where the latter is more robust to contamination. These challenges have motivated many researchers to propose alternative estimation techniques for a wide range of distributions; see, for example, [10–13], among other studies.

This paper investigates the performance of nine frequentist estimation methods for the change point of the BS hazard rate and examines their robustness in the presence of data contamination. Here, data contamination refers to the occurrence of outliers, extreme values, or both. The BS distribution is a lifetime model, that is, a probability distribution with positive support commonly used to fit time-to-event data in reliability and survival studies. A positive continuous random variable T is said to follow a BS distribution with shape parameter α and scale parameter β (denoted as $T \sim \mathrm{BS}(\alpha, \beta)$) if its cumulative distribution function (CDF) is given by

$$F(t;\alpha,\beta) = \Phi\left(\frac{1}{\alpha}\left[\sqrt{\frac{t}{\beta}} - \sqrt{\frac{\beta}{t}}\right]\right), \quad t > 0,\ \alpha > 0,\ \beta > 0, \tag{1.1}$$

where $\Phi(\cdot)$ denotes the standard normal CDF. Accordingly, the probability density function (PDF) and

hazard function (HF) of the BS distribution are expressed as

$$f(t;\alpha,\beta) = \frac{1}{2\alpha t}\left[\sqrt{\frac{t}{\beta}} + \sqrt{\frac{\beta}{t}}\right]\phi\left(\frac{1}{\alpha}\left[\sqrt{\frac{t}{\beta}} - \sqrt{\frac{\beta}{t}}\right]\right) \tag{1.2}$$

and

$$h(t;\alpha,\beta) = \frac{f(t;\alpha,\beta)}{1-F(t;\alpha,\beta)} = \frac{\frac{1}{2\alpha t}\left[\sqrt{\frac{t}{\beta}} + \sqrt{\frac{\beta}{t}}\right]\phi\left(\frac{1}{\alpha}\left[\sqrt{\frac{t}{\beta}} - \sqrt{\frac{\beta}{t}}\right]\right)}{\Phi\left[\frac{1}{\alpha}\left(\sqrt{\frac{t}{\beta}} - \sqrt{\frac{\beta}{t}}\right)\right]}, \tag{1.3}$$

respectively, where $t > 0$, $\alpha > 0$, $\beta > 0$, and $\phi(\cdot)$ is the standard normal PDF.

Using Eq (1.1), the quantile function of the BS distribution can be written as

$$Q(u;\alpha,\beta) = \frac{\beta}{4}\left[\alpha\Phi^{-1}(u) + \sqrt{4 + \{\alpha\Phi^{-1}(u)\}^2}\right]^2, \tag{1.4}$$

where $0 < u < 1$, $\alpha > 0$, $\beta > 0$, and $\Phi^{-1}(\cdot)$ denotes the standard normal quantile function. This quantile function is useful for simulating random variates from the BS distribution and for deriving its distributional properties (e.g., moments and median); see, for example, [14].

The BS distribution has a close relationship with the normal distribution and possesses several desirable features. Since its introduction by [15, 16] over five decades ago, it has attracted considerable attention. Extensive research has been devoted to its physical interpretations [17], generalizations [18, 19], inferential procedures [20, 21], and multivariate extensions [22–25]. Comprehensive reviews can be found in [14], while some recent applications were documented in [26–30]. The PDF and HF of the BS distribution are unimodal for all parameter values; see Figures 1 and 2. In the literature, HFs are often assumed to be constant (as in the exponential distribution) or monotonic (as in the Weibull distribution). In practice, however, the HF can be non-monotonic, as is the case for the BS distribution. A unimodal HF increases up to a certain time point, known as the change point, and subsequently decreases, eventually stabilizing. For example, in a study on breast cancer recovery, [31] observed a unimodal HF, where the highest mortality rate occurred approximately three years after diagnosis, after which the mortality rate declined gradually. Three well-known distributions with unimodal HFs are the log-normal, inverse Gaussian, and BS distributions. It is noteworthy that the BS hazard curve converges to a positive constant, unlike the log-normal and inverse Gaussian distributions, for which the HF tends to zero; see [32].

This paper investigates the performance of nine frequentist estimation methods for the change point of the BS hazard rate and examines their robustness in the presence of data contamination (i.e., occurrence of outliers, extreme values, or both). The estimators considered for the model parameters include the modified moments estimators (MMEs), maximum likelihood estimators (MLEs), three least-squares-based estimators, the maximum product of spacings estimators (MPSEs), and three minimum-distance-based estimators. The objective of this study is to explore and identify the most effective estimation method among these alternatives, as this topic is of considerable interest to applied statisticians and reliability engineers. It is worth noting that although some of these methods may outperform MLEs and MPSEs in finite samples, they may not necessarily possess favorable asymptotic or distributional properties.

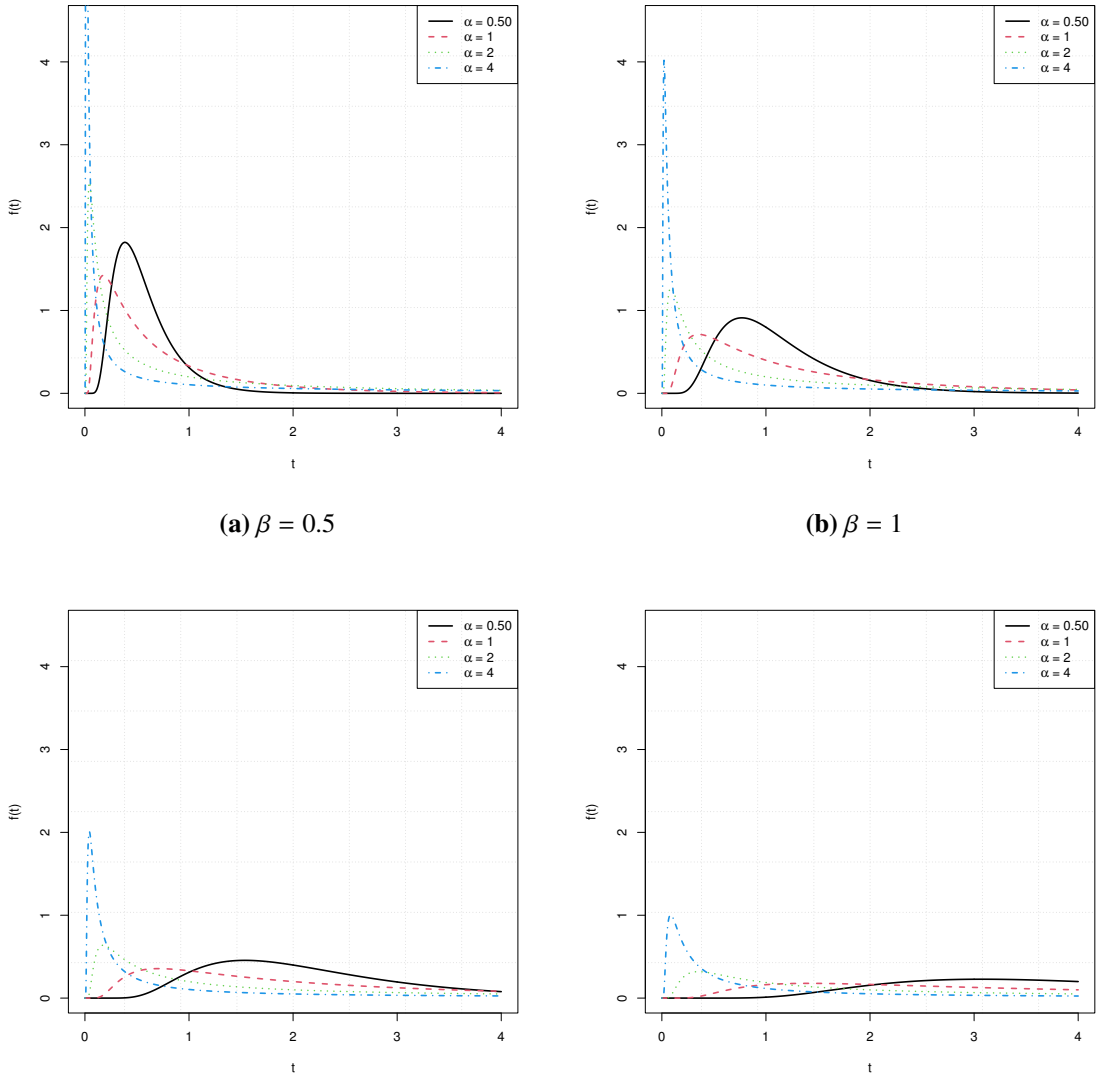

(a) $\beta = 0.5$ **(b)** $\beta = 1$

(c) $\beta = 2$ **(d)** $\beta = 4$

Figure 1. The PDF of the BS distribution for various values of the shape parameter α and the scale parameter β.

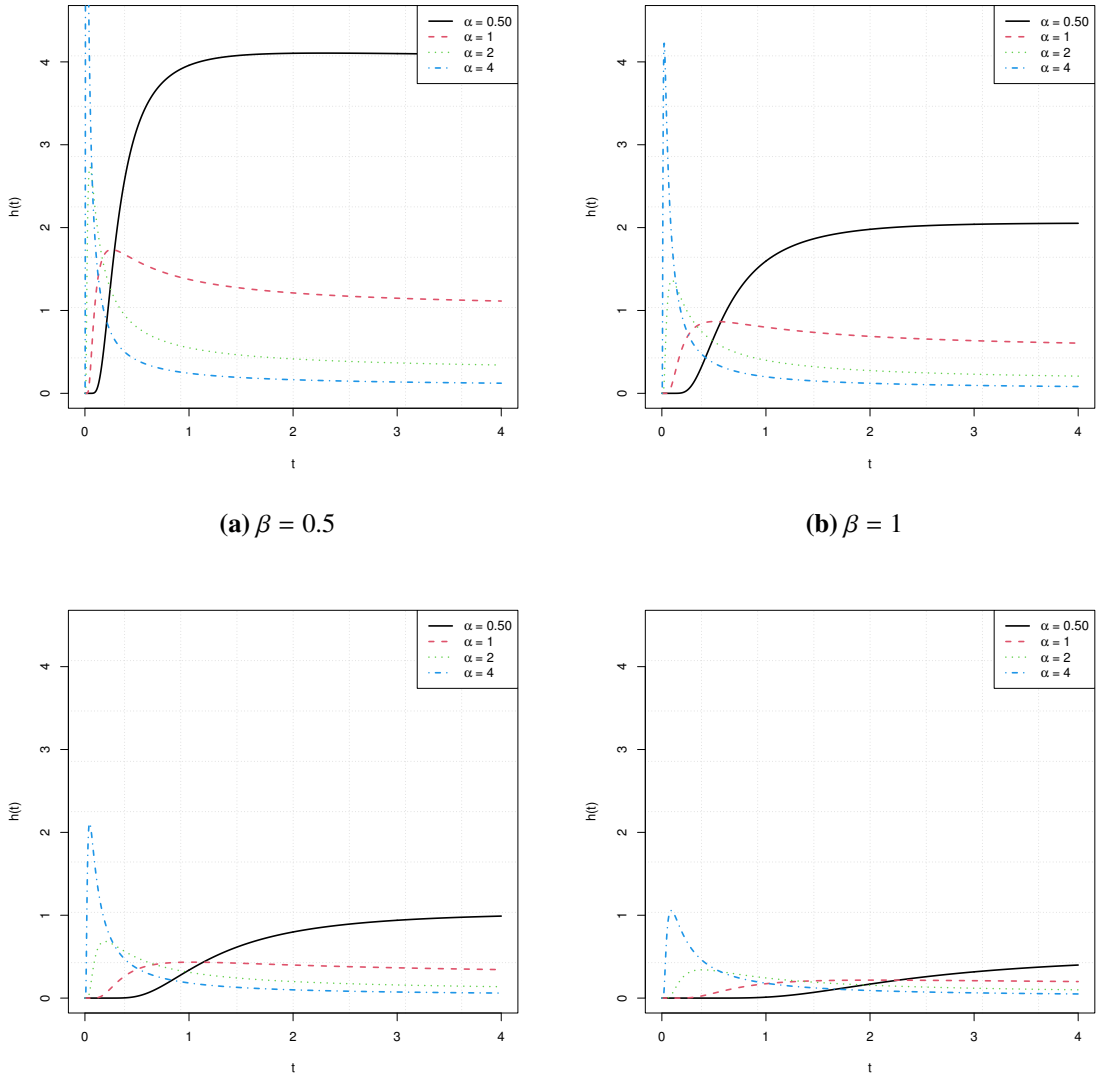

(a) $\beta = 0.5$ **(b)** $\beta = 1$

(c) $\beta = 2$ **(d)** $\beta = 4$

Figure 2. The HF of the BS distribution for various values of the shape parameter α and the scale parameter β.

The remainder of this paper is organized as follows. Section 2 provides details of the nine estimation methods under consideration. Section 3 presents the results of extensive Monte Carlo simulations designed to compare the performance of the estimators under various conditions. Section 4 illustrates the application of the proposed methods to a real biomedical dataset. Finally, Section 5 concludes the paper with a summary of findings and directions for future research.

2. Change point estimation

Recall that Eq (1.3) is the HF of the BS distribution and β is a positive scale parameter. Accordingly, and based on [1], the change point of the HF is $c_{\alpha,\beta}$, such that $c_{\alpha,\beta} = \beta c_\alpha$. Here, c_α is a decreasing

function of α and the solution of the following nonlinear equation:

$$\alpha\left[\epsilon'(t)\right]^2\phi\left(-\frac{\epsilon(t)}{\alpha}\right)+\left\{\alpha^2\epsilon''(t)-\epsilon(t)\left[\epsilon'(t)\right]^2\right\}\Phi\left(-\frac{\epsilon(t)}{\alpha}\right)=0, \tag{2.1}$$

such that $\Phi(\cdot)$ is the standard normal CDF, $\phi(\cdot)$ is the standard normal PDF,

$$\epsilon(t)=t^{\frac{1}{2}}-t^{-\frac{1}{2}},\ \epsilon'(t)=\frac{1}{2t}\left(t^{\frac{1}{2}}+t^{-\frac{1}{2}}\right),\ \text{and}\ \epsilon''(t)=-\frac{1}{4t^2}\left(t^{\frac{1}{2}}+3t^{-\frac{1}{2}}\right).$$

Clearly, since Eq (2.1) is nonlinear; thus, one must use numerical means to approximate the solution. However, for small values of the shape parameter, the approximation might not be stable when one uses standard root solving techniques (e.g., Newton's method) as indicated in [1]. The following parts of this section discuss nine approaches to estimate the model parameters from which one can estimate the change point.

2.1. Modified moments estimation

In statistical literature, the method of moments is one of the oldest estimation technique commonly to acquire closed-form estimators for the model parameters. In [20], MMEs were obtained rather than those obtained using the conventional approach. [1] made use of the MMEs to estimate the change point $c_{\alpha,\beta}$ since they are easy to calculate due to their closed-form expressions, and their behavior is very similar to the MLEs. However, their performance is still unknown when data contamination exists. If $t_1,\ldots,t_n$ represent the observed random sample of size n from BS(α,β), then based on the its distributional properties, the MMEs of α and β are given by

$$\hat{\alpha}_{\text{MME}}=\sqrt{2\left[\left(\frac{s}{r}\right)^{\frac{1}{2}}-1\right]} \tag{2.2}$$

and

$$\hat{\beta}_{\text{MME}}=\sqrt{sr}, \tag{2.3}$$

respectively, such that:

$$s=\frac{1}{n}\sum_{i=1}^{n}t_i\quad\text{and}\quad r=\left[\frac{1}{n}\sum_{i=1}^{n}t_i^{-1}\right]^{-1}$$

are the sample arithmetic and harmonic means, respectively. The MMEs were considered to estimate the BS distribution based on the Laplace kernel by [33].

2.2. Maximum likelihood estimation

Recall that $t_1,\ldots,t_n$ represents the observed random sample of size n from BS(α,β) with probability density function (1.2). The MLEs of the model parameters were originally obtained in [15, 16], while their asymptotic distributions were derived in [34]. The existence and uniqueness of the MLEs were proved in [35]. Let

$$K(\beta)=\left[\frac{1}{n}\sum_{i=1}^{n}(t_i+\beta)^{-1}\right]^{-1}$$

be a harmonic mean function, such that $K(0) = r$. The MLE of β, which is denoted by $\hat{\beta}_{\text{MLE}}$, can be obtained as the unique positive root of the following nonlinear equation:

$$\beta^2 - \beta\,[2r + K(\beta)] + r\,[s + K(\beta)] = 0. \tag{2.4}$$

Once $\hat{\beta}_{\text{MLE}}$ is numerically determined as a solution of (2.4), the MLE of α, which is denoted by $\hat{\alpha}_{\text{MLE}}$, can be obtained explicitly as

$$\hat{\alpha}_{\text{MLE}} = \sqrt{\frac{s}{\hat{\beta}_{\text{MLE}}} + \frac{\hat{\beta}_{\text{MLE}}}{r} - 2}. \tag{2.5}$$

Note that r and s are defined as shown in the aforementioned subsection.

2.3. Least-squares estimation

The first type of least-squares-based estimator is the least-squares estimator (LSE), which was initially considered in [36] to estimate the parameters of the beta distribution. Suppose that $t_{1:n} < \ldots < t_{n:n}$ are the corresponding observed order statistics based on a random sample $t_1, \ldots, t_n$ of size n from an arbitrary probability distribution with CDF $F(t)$. It is known that:

$$\mathrm{E}\,[F(t_{i:n})] = \frac{i}{n+1},$$

since $F(t_{1:n}), \ldots, F(t_{n:n})$ are order statistics from a standard uniform distribution; see, for example, [37]. The LSEs of α and β; say, $\hat{\alpha}_{\text{LSE}}$ and $\hat{\beta}_{\text{LSE}}$, respectively, are obtained by minimizing the following least-squares objective function:

$$S(\alpha,\beta) = \sum_{i=1}^{n}\left[\Phi\left(\frac{1}{\alpha}\left[\sqrt{\frac{t_{i:n}}{\beta}} - \sqrt{\frac{\beta}{t_{i:n}}}\right]\right) - \frac{i}{n+1}\right]^2. \tag{2.6}$$

The first-order derivatives of Eq (2.6) with respect to the model parameters are as follows:

$$\frac{\partial S}{\partial \alpha} = 2\sum_{i=1}^{n}\left[\Phi\left(\frac{1}{\alpha}\left[\sqrt{\frac{t_{i:n}}{\beta}} - \sqrt{\frac{\beta}{t_{i:n}}}\right]\right) - \frac{i}{n+1}\right]\partial_\alpha(t_{i:n})$$

and

$$\frac{\partial S}{\partial \beta} = 2\sum_{i=1}^{n}\left[\Phi\left(\frac{1}{\alpha}\left[\sqrt{\frac{t_{i:n}}{\beta}} - \sqrt{\frac{\beta}{t_{i:n}}}\right]\right) - \frac{i}{n+1}\right]\partial_\beta(t_{i:n}),$$

such that

$$\partial_\alpha(t) = -\frac{A(t;\beta)}{\alpha^2}\phi\left(\frac{A(t;\beta)}{\alpha}\right) \tag{2.7}$$

and

$$\partial_\beta(t) = -\frac{B(t;\beta)}{2\alpha\beta}\phi\left(\frac{A(t;\beta)}{\alpha}\right), \tag{2.8}$$

where

$$A(t;\beta) = \frac{t-\beta}{\sqrt{\beta t}}, \tag{2.9}$$

$$B(t;\beta) = \frac{t+\beta}{\sqrt{\beta t}}, \tag{2.10}$$

and $\phi(\cdot)$ is the standard normal PDF. It is important to mention that Eq (2.7) to Eq (2.10) are frequntly used in the following subsection.

2.4. Weighted least squares estimation

The second type of least-squares-based estimator is the weighted least-squares estimator (WLSE), which was also considered in [36]. Both LSEs and their weighted counterparts were later used in [5–8]. Recall that $t_{1:n} < \ldots < t_{n:n}$ are the corresponding observed order statistics based on a random sample $t_1, \ldots, t_n$ of size n. Since $F(t_{1:n}), \ldots, F(t_{n:n})$ are order statistics form a standard uniform distribution, then it is also known that:

$$\text{Var}\left[F(t_{i:n})\right] = \frac{i(n-i+1)}{(n+1)^2(n+1)};$$

see [37] for more details. The WLSEs of α and β; say, $\hat{\alpha}_{\text{WLSE}}$ and $\hat{\beta}_{\text{WLSE}}$, respectively, are obtained by minimizing the following weighted least-squares objective function:

$$S_w(\alpha,\beta) = \sum_{i=1}^{n} w_i \left[\Phi\left(\frac{1}{\alpha}\left[\sqrt{\frac{t_{i:n}}{\beta}} - \sqrt{\frac{\beta}{t_{i:n}}}\right]\right) - \frac{i}{n+1}\right]^2, \tag{2.11}$$

where $w_{1:n}, \ldots, w_{n:n}$ are the weights of $t_{1:n} < \ldots < t_{n:n}$, respectively, such that

$$w_{i:n} = \frac{(n+1)^2(n+1)}{i(n-i+1)}.$$

The first-order derivatives of Eq (2.11) with respect to the model parameters are as follows:

$$\frac{\partial S_w}{\partial \alpha} = 2\sum_{i=1}^{n} w_{i:n}\left[\Phi\left(\frac{1}{\alpha}\left[\sqrt{\frac{t_{i:n}}{\beta}} - \sqrt{\frac{\beta}{t_{i:n}}}\right]\right) - \frac{i}{n+1}\right]\partial_\alpha(t_{i:n})$$

and

$$\frac{\partial S_w}{\partial \beta} = 2\sum_{i=1}^{n} w_{i:n}\left[\Phi\left(\frac{1}{\alpha}\left[\sqrt{\frac{t_{i:n}}{\beta}} - \sqrt{\frac{\beta}{t_{i:n}}}\right]\right) - \frac{i}{n+1}\right]\partial_\beta(t_{i:n}).$$

2.5. Percentile estimation

The third least-squares-based estimator is obtained as follows. When data comes from a population with a closed-form CDF and QF, then one may estimate the unknown model parameters by fitting a linear model to the theoretical percentiles obtained from the QF and the sample percentiles. This method was proposed in [38, 39]. Examples of its usage are found in [5, 6, 40]. Recall that $t_{1:n} < \ldots < t_{n:n}$ are the corresponding realizations of the order statistics based on a random sample $t_1, \ldots, t_n$ of size n. Based on Eq (1.4), and if $F(t_{i:n}; \alpha, \beta)$ are estimated by $p_{i:n} = \text{E}\left[F(t_{i:n})\right]$ for $i = 1, \ldots, n$, then the percentile estimators of α and β; say, $\hat{\alpha}_{\text{PCE}}$ and $\hat{\beta}_{\text{PCE}}$, can be obtained by minimizing:

$$S_p = \sum_{i=1}^{n}\left\{t_{i:n} - \frac{\beta}{4}\left[\alpha\Phi^{-1}(p_{i:n}) + \sqrt{4 + \{\alpha\Phi^{-1}(p_{i:n})\}^2}\right]^2\right\}^2 \tag{2.12}$$

where $p_{i:n} = \frac{i}{n+1}$. The first-order derivatives of Eq (2.12) with respect to the model parameters are as follows:

$$\frac{\partial S_p}{\partial \alpha} = 2\sum_{i=1}^{n}\left\{t_{i:n} - \frac{\beta}{4}\left[\alpha\Phi^{-1}(p_{i:n}) + \sqrt{4 + \{\alpha\Phi^{-1}(p_{i:n})\}^2}\right]^2\right\} q_\alpha(p_{i:n}),$$

and

$$\frac{\partial S_{\,p}}{\partial \beta} = 2\sum_{i=1}^{n}\left\{t_{i:n} - \frac{\beta}{4}\left[\alpha\Phi^{-1}(p_{i:n}) + \sqrt{4 + \{\alpha\Phi^{-1}(p_{i:n})\}^2}\right]^2\right\} q_\beta(p_{i:n}),$$

such that

$$q_\alpha(u) = -2\frac{\Phi^{-1}(u)Q(u;\alpha,\beta)}{\sqrt{4 + [\alpha\Phi^{-1}(u)]^2}}$$

and

$$q_\beta(u) = -Q(u;\alpha,1),$$

where $Q(u;\alpha,\beta)$ is given by Eq (1.4).

2.6. Maximum product of spacings estimation

Recent research indicates that MPSEs currently rival MLEs in terms of estimation efficiency. They were formally introduced in [41–43]. MPSEs belong to a class of a more general estimation method using spacings; see in this connection [44]. If $t_{1:n} < \ldots < t_{n:n}$ are the observed order statistics based on a random sample of size n, then the MPSEs for the model parameters; say, $\hat{\alpha}_{\text{MPSE}}$ and $\hat{\beta}_{\text{MPSE}}$, are acquired by maximizing:

$$P = \frac{1}{n+1}\sum_{i=1}^{n+1}\log\Delta_i, \tag{2.13}$$

such that

$$\Delta_i = \begin{cases} \Phi\left(\frac{1}{\alpha}\left[\sqrt{\frac{t_{1:n}}{\beta}} - \sqrt{\frac{\beta}{t_{1:n}}}\right]\right) & \text{if } i = 1, \\ \Phi\left(\frac{1}{\alpha}\left[\sqrt{\frac{t_{i:n}}{\beta}} - \sqrt{\frac{\beta}{t_{i:n}}}\right]\right) - \Phi\left(\frac{1}{\alpha}\left[\sqrt{\frac{t_{i-1:n}}{\beta}} - \sqrt{\frac{\beta}{t_{i-1:n}}}\right]\right) & \text{if } 1 < i \le n, \\ \Phi\left(-\frac{1}{\alpha}\left[\sqrt{\frac{t_{n:n}}{\beta}} - \sqrt{\frac{\beta}{t_{n:n}}}\right]\right) & \text{if } i = n+1. \end{cases}$$

The first-order derivatives of Eq (2.13) with respect to the model parameters are as follows:

$$\frac{\partial P}{\partial \alpha} = \frac{1}{n+1}\sum_{i=1}^{n+1}\frac{\partial_\alpha\Delta_i}{\Delta_i}$$

and

$$\frac{\partial P}{\partial \beta} = \frac{1}{n+1}\sum_{i=1}^{n+1}\frac{\partial_\beta\Delta_i}{\Delta_i},$$

where

$$\partial_\alpha\Delta_i = \begin{cases} \partial_\alpha(t_{1:n}) & \text{if } i = 1, \\ \partial_\alpha(t_{i:n}) - \partial_\alpha(t_{i-1:n}) & \text{if } 1 < i \le n, \\ -\partial_\alpha(t_{n:n}) & \text{if } i = n+1, \end{cases}$$

and

$$\partial_\beta\Delta_i = \begin{cases} \partial_\beta(t_{1:n}) & \text{if } i = 1, \\ \partial_\beta(t_{i:n}) - \partial_\beta(t_{i-1:n}) & \text{if } 1 < i \le n, \\ -\partial_\beta(t_{n:n}) & \text{if } i = n+1. \end{cases}$$

2.7. Cramér-von Mises estimation

The Cramér-von Mises method belongs to the class of minimum distance methods, and the corresponding CVMEs; say, $\hat{\alpha}_{\text{CVME}}$ and $\hat{\beta}_{\text{CVME}}$, are found by minimizing:

$$C = \frac{1}{12n} + \sum_{i=1}^{n}\left[\Phi\left(\frac{1}{\alpha}\left[\sqrt{\frac{t_{i:n}}{\beta}} - \sqrt{\frac{\beta}{t_{i:n}}}\right]\right) - \frac{2i-1}{2n}\right]^2, \tag{2.14}$$

such that $t_{1:n} < \ldots < t_{n:n}$ are the observed order statistics of a random sample of size n. Moreover, the first-order derivatives of Eq (2.14) with respect to the model parameters are as follows:

$$\frac{\partial C}{\partial \alpha} = 2\sum_{i=1}^{n}\left[\Phi\left(\frac{1}{\alpha}\left[\sqrt{\frac{t_{i:n}}{\beta}} - \sqrt{\frac{\beta}{t_{i:n}}}\right]\right) - \frac{2i-1}{2n}\right]\partial_\alpha(t_{i:n})$$

and

$$\frac{\partial C}{\partial \beta} = 2\sum_{i=1}^{n}\left[\Phi\left(\frac{1}{\alpha}\left[\sqrt{\frac{t_{i:n}}{\beta}} - \sqrt{\frac{\beta}{t_{i:n}}}\right]\right) - \frac{2i-1}{2n}\right]\partial_\beta(t_{i:n}).$$

2.8. Anderson-Darling estimation

Anderson-Darling estimation and its right-tailed version also belong to the class of minimum distance methods. In this subsection, the former is considered, while the latter is discussed in the following subsection. Based on the fact that $t_{1:n} < \ldots < t_{n:n}$, then the ADEs for the model parameters; say, $\hat{\alpha}_{\text{ADE}}$ and $\hat{\beta}_{\text{ADE}}$, are determined by minimizing:

$$\begin{aligned} A = -n &- \frac{1}{n}\sum_{i=1}^{n}(2i-1)\log\Phi\left(-\frac{1}{\alpha}\left[\sqrt{\frac{t_{n-i+1:n}}{\beta}} - \sqrt{\frac{\beta}{t_{n-i+1:n}}}\right]\right) \\ &- \frac{1}{n}\sum_{i=1}^{n}(2i-1)\log\Phi\left(\frac{1}{\alpha}\left[\sqrt{\frac{t_{i:n}}{\beta}} - \sqrt{\frac{\beta}{t_{i:n}}}\right]\right). \end{aligned} \tag{2.15}$$

The first-order derivatives of Eq (2.15) with respect to the model parameters are as follows:

$$\begin{aligned} \frac{\partial A}{\partial \alpha} &= \frac{1}{n}\sum_{i=1}^{n}(2i-1)\frac{\partial_\alpha(t_{n-i+1:n})}{\Phi\left(-\frac{1}{\alpha}\left[\sqrt{\frac{t_{n-i+1:n}}{\beta}} - \sqrt{\frac{\beta}{t_{n-i+1:n}}}\right]\right)} \\ &\quad -\frac{1}{n}\sum_{i=1}^{n}(2i-1)\frac{\partial_\alpha(t_{i:n})}{\Phi\left(\frac{1}{\alpha}\left[\sqrt{\frac{t_{i:n}}{\beta}} - \sqrt{\frac{\beta}{t_{i:n}}}\right]\right)} \end{aligned}$$

and

$$\begin{aligned} \frac{\partial A}{\partial \beta} &= \frac{1}{n}\sum_{i=1}^{n}(2i-1)\frac{\partial_\beta(t_{n-i+1:n})}{\Phi\left(-\frac{1}{\alpha}\left[\sqrt{\frac{t_{n-i+1:n}}{\beta}} - \sqrt{\frac{\beta}{t_{n-i+1:n}}}\right]\right)} \\ &\quad -\frac{1}{n}\sum_{i=1}^{n}(2i-1)\frac{\partial_\beta(t_{i:n})}{\Phi\left(\frac{1}{\alpha}\left[\sqrt{\frac{t_{i:n}}{\beta}} - \sqrt{\frac{\beta}{t_{i:n}}}\right]\right)}. \end{aligned}$$

2.9. Right-tailed Anderson-Darling estimation

From a random sample of size n, and based on the corresponding observed order statistics $t_{1:n} < \ldots < t_{n:n}$, then the RADEs for the model parameters; say, $\hat{\alpha}_{\text{RADE}}$ and $\hat{\beta}_{\text{RADE}}$, are determined by minimizing:

$$A_R = \frac{n}{2} - \frac{1}{n}\sum_{i=1}^{n}(2i-1)\log\Phi\left(-\frac{1}{\alpha}\left[\sqrt{\frac{t_{n-i+1:n}}{\beta}} - \sqrt{\frac{\beta}{t_{n-i+1:n}}}\right]\right) - 2\sum_{i=1}^{n}\Phi\left(\frac{1}{\alpha}\left[\sqrt{\frac{t_{i:n}}{\beta}} - \sqrt{\frac{\beta}{t_{i:n}}}\right]\right). \tag{2.16}$$

The first-order derivatives of Eq (2.16) with respect to the model parameters are as follows:

$$\frac{\partial A_R}{\partial \alpha} = \frac{1}{n}\sum_{i=1}^{n}(2i-1)\frac{\partial_\alpha(t_{n-i+1:n})}{\Phi\left(-\frac{1}{\alpha}\left[\sqrt{\frac{t_{n-i+1:n}}{\beta}} - \sqrt{\frac{\beta}{t_{n-i+1:n}}}\right]\right)} - 2\sum_{i=1}^{n}\partial_\alpha(t_{i:n})$$

and

$$\frac{\partial A_R}{\partial \beta} = \frac{1}{n}\sum_{i=1}^{n}(2i-1)\frac{\partial_\beta(t_{n-i+1:n})}{\Phi\left(-\frac{1}{\alpha}\left[\sqrt{\frac{t_{n-i+1:n}}{\beta}} - \sqrt{\frac{\beta}{t_{n-i+1:n}}}\right]\right)} - 2\sum_{i=1}^{n}\partial_\beta(t_{i:n}).$$

3. Numerical illustrations and simulations

This section is divided into two parts. The first presents an illustrative example that demonstrates the performance of the proposed estimation methods for determining the change point. The second reports the results of a Monte Carlo simulation study aimed at comparing the efficiency and robustness of the considered estimators under various contaminated data scenarios.

3.1. Illustrative example

Suppose that the change point is estimated based on a data set of size 10 (i.e., $n = 10$) simulated from BS(1.5, 1.0) and is reported in Table 1. The actual change point $c_{\alpha,\beta}$ is found to be approximately equal to 0.185. Before obtaining estimators for the model parameters, one must check their existence and uniqueness. Mathematically proving these requirements is beyond this study's scope; nevertheless, one may prove them using graphical means. Using extensive Monte Carlo simulations, a three-dimensional (3D) plot for the profile of each objective function of each estimation method is established, as shown in Figures 3 and 4. These 3D surfaces serve as visual diagnostics, analogous to contour plots. The 3D charts clearly indicate that global extrema exist and are unique. The MMEs for α and β are first calculated and then used as initial values to acquire the remaining estimators.

Table 1. Simulated data from BS(1.5, 1.0).

0.44143	0.70923	7.33011	1.11150	1.21365
8.50062	1.97052	0.03693	0.37179	0.51859

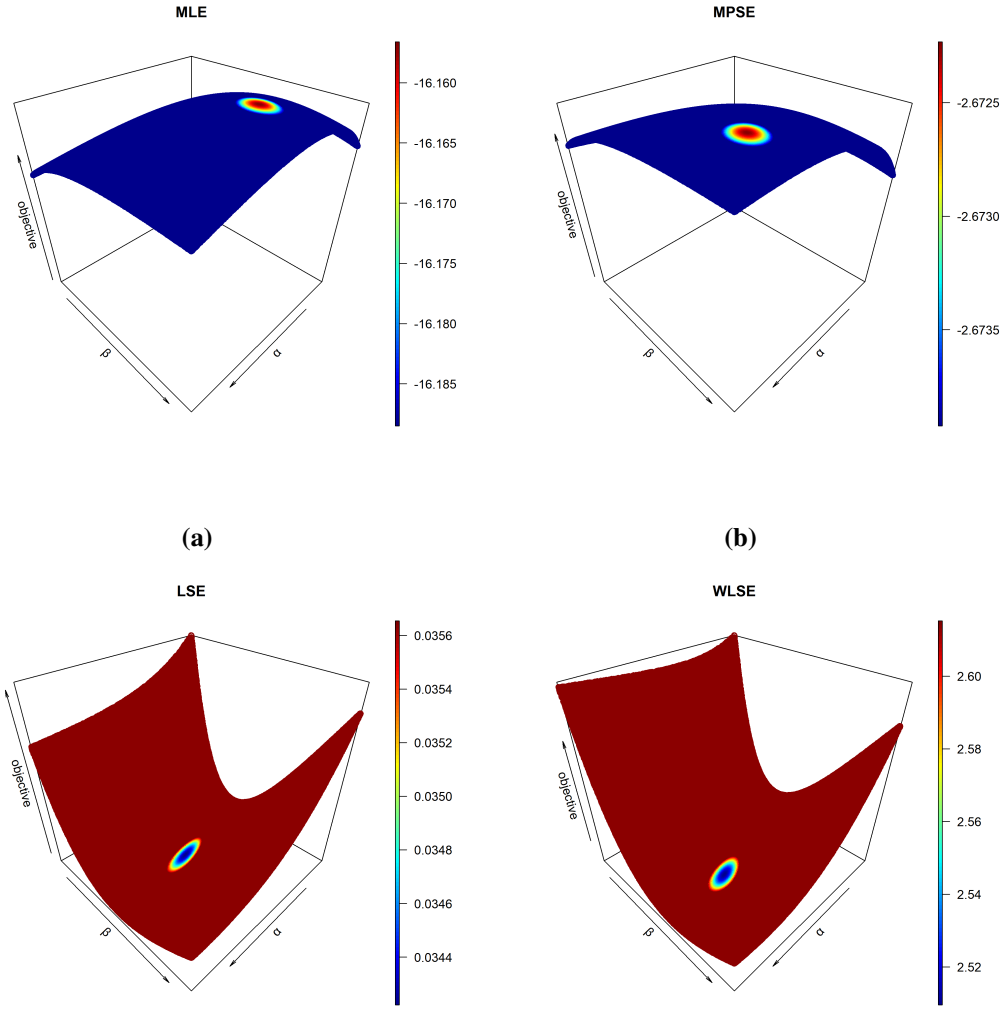

Figure 3. 3D surface plots of the objective functions for the nine estimation methods applied to the simulated BS(1.5, 1.0) dataset (Table 1). The localized peak in each plot confirms the existence of a unique optimum.

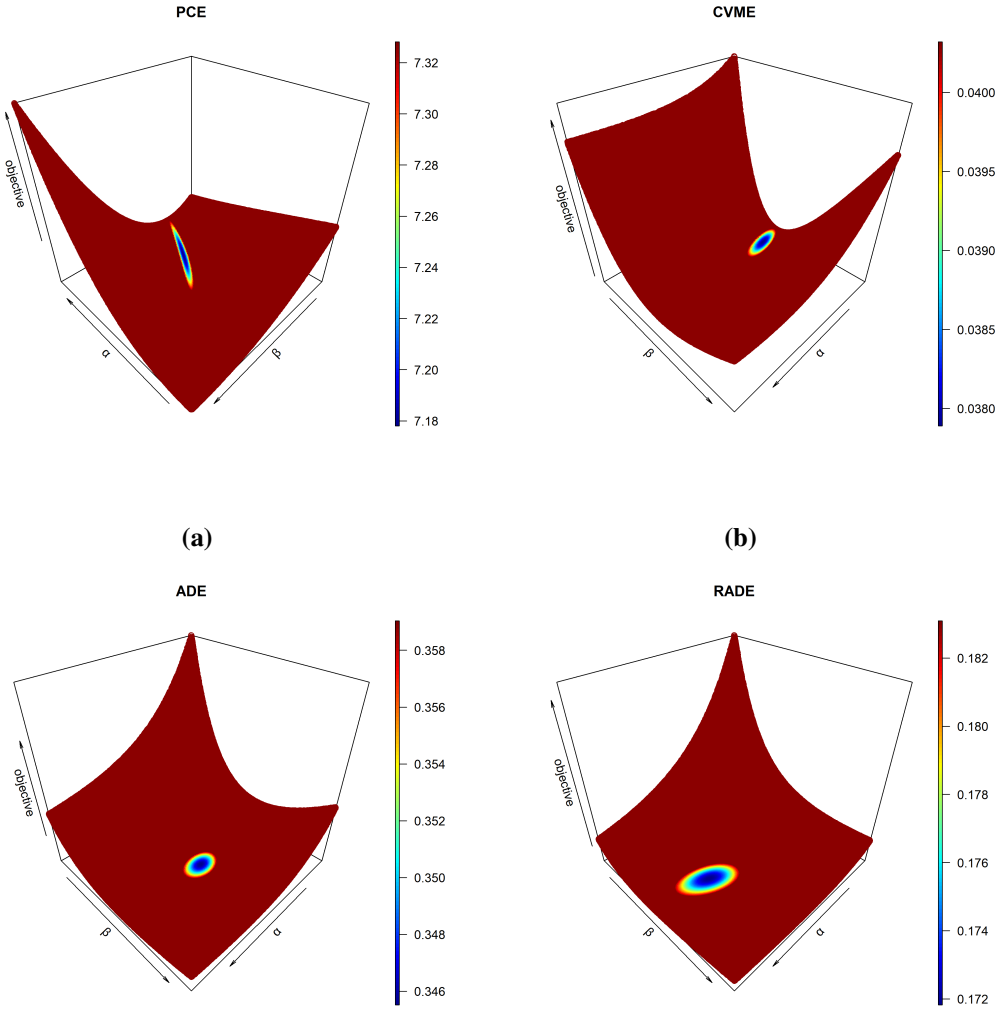

Figure 4. 3D surface plots of the objective functions for the nine estimation methods applied to the simulated BS(1.5, 1.0) dataset (Table 1). The localized peak in each plot confirms the existence of a unique optimum (cont.).

Accordingly, nine estimates are found for the change point $c_{\alpha,\beta}$ as summarized in Table 2 alongside the estimators of the model parameters. From the latter table, one can easily observe that MPSE and WLSE of $c_{\alpha,\beta}$ provided the closest approximations for the change point.

Table 2. Estimation of $c_{\alpha,\beta}$ using nine methods based on data in Table 1.

Method	$\hat{\alpha}$	$\hat{\beta}$	$c_{\hat{\alpha},\hat{\beta}}$
MME	1.344	1.175	0.282
MLE	1.344	1.217	0.292
LSE	1.506	0.961	0.176
WLSE	1.620	1.047	0.162
PCE	2.169	0.897	0.073
MPSE	1.683	1.243	0.177
CVME	1.162	0.907	0.313
ADE	1.499	1.069	0.198
RADE	1.694	1.012	0.142

3.2. Simulation outcomes

Consider the following data contamination scenarios:

(S1) No contamination.
(S2) Severe upper contamination, where the upper 10% of order statistics are multiplied by 5.
(S3) Severe lower contamination, where the lower 10% of order statistics are multiplied by $1/5$.
(S4) Severe two-tailed contamination, where the upper 10% of order statistics are multiplied by 5 and the lower 5% of order statistics are multiplied by $1/5$.

These scenarios are inspired by [13]. For each case, 10,000 random samples of sizes {10, 20, 30, 40, 50, 60, 70, 80, 90, 100} are generated with model parameters $\alpha = 0.5, 1, 2$. These choices are intended to numerically examine the effect of increasing both sample size and shape parameter value on estimation efficiency. Simulation studies often assume that estimators are scale invariant (see, e.g., [6]); therefore, without loss of generality, the true value of the scale parameter β is set equal to one in all simulation settings. It is important to note that β is not assumed to be known in the estimation; rather, it is estimated from the simulated samples under each method. The corresponding critical values for these parameters are $c_{0.5,1} = 4.572471$, $c_{1,1} = 0.5148967$, and $c_{2,1} = 0.09678019$, respectively.

For each simulation, the bias and root mean squared error (RMSE) of the estimated critical values are computed as

$$\text{Bias}(c_{\hat{\alpha},\hat{\beta}}) = \frac{1}{M}\sum_{i=1}^{M}(\hat{c}_i - c_{\alpha,\beta})$$

and

$$\text{RMSE}(c_{\hat{\alpha},\hat{\beta}}) = \sqrt{\frac{1}{M}\sum_{i=1}^{M}(\hat{c}_i - c_{\alpha,\beta})^2},$$

where M is the number of simulation runs and $\hat{c}_i = c_{\hat{\alpha}_i,\hat{\beta}_i}$ denotes the estimated critical value in run i, with $\hat{\alpha}_i$ and $\hat{\beta}_i$ being any of the considered estimators.

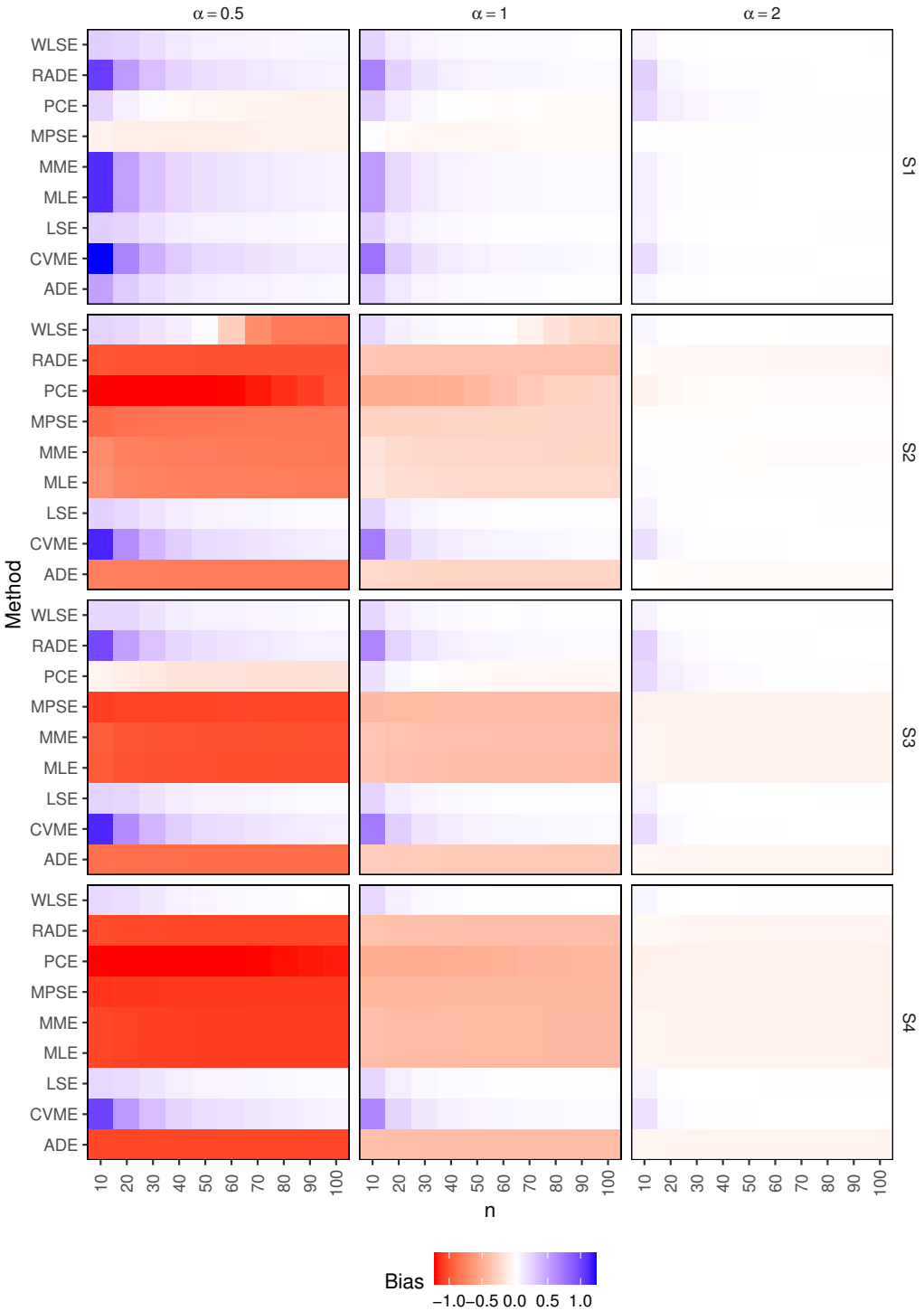

Figure 5. Bias of nine estimators of the BS hazard change point $c_{\alpha,\beta}$ under four data contamination scenarios: (S1) no contamination; (S2) upper-tail; (S3) lower-tail; and (S4) two-tailed contamination. Results are shown for $\alpha = 0.5, 1, 2$ across increasing sample sizes ($n = 10, 20, \ldots, 100$). CVME, LSE, and WLSE exhibit the smallest bias, particularly under data contamination.

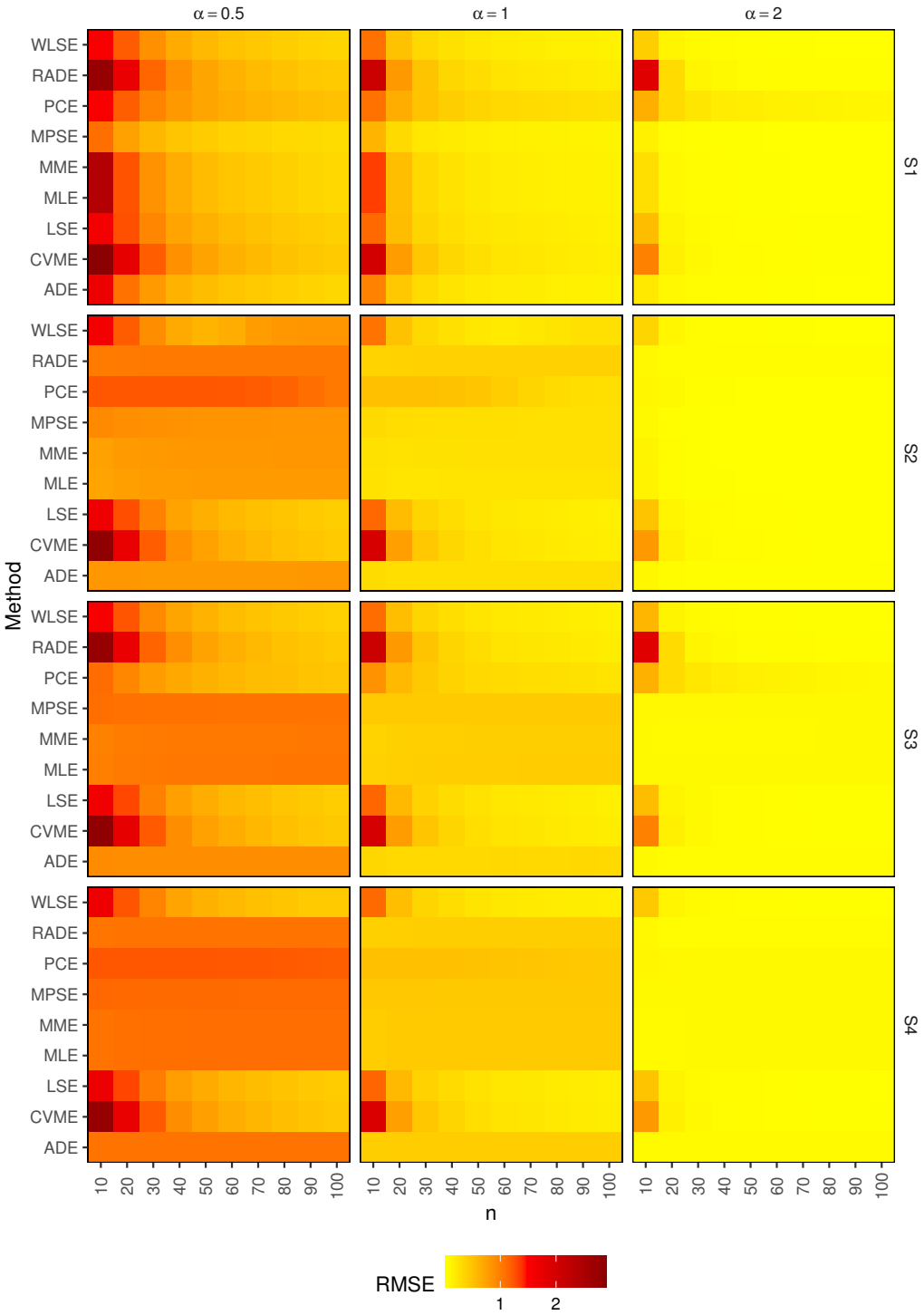

Figure 6. Root mean squared error (RMSE) of nine estimators of the BS hazard change point $c_{\alpha,\beta}$ under the same data contamination scenarios as in Figure 5. As the sample size increases, RMSE decreases across all methods. CVME, LSE, and WLSE show the most robust performance under data contamination.

All numerical results were obtained using **R**, an environment for statistical computing [45].* Figures 5 and 6 display the outcomes of the simulation study. The following observations can be made:

(1) As the sample size increases, the RMSEs decrease across all estimation methods, indicating consistency of the estimators.
(2) Biases approach zero with larger samples, confirming asymptotic unbiasedness.
(3) Under contaminated data, some estimators such as MME, MLE, PCE, MPSE, ADE, and RADE exhibited poor performance for small shape parameter values and small sample sizes, as reflected in larger bias and RMSE values. By contrast, the performance of CVMEs, LSEs, and WLSEs improves with larger samples.
(4) As the shape parameter increases, all methods converge in performance in terms of both bias and RMSE, regardless of contamination.
(5) Performance tends to deteriorate as the proportion of contamination increases, except for CVMEs, LSEs, and WLSEs, which demonstrate greater robustness.

4. Application

The practical application of the considered estimators is illustrated using a real dataset. This dataset comprises 72 lifetimes (in days), shown in Table 3, of guinea pigs (cavia porcellus) injected with different dosages of Mycobacterium tuberculosis, a pathogenic bacterium that causes tuberculosis. This dataset has previously been analyzed in [1, 3], among others. Onec again, extensive Monte Carlo simulations were conducted to construct three-dimensional (3D) profiles of the objective functions for each estimation method based on data in Table 3, as illustrated in Figures 7 and 8. As previously mentioned, these surfaces act as visual diagnostics, similar in purpose to contour plots. The 3D charts clearly reveal the existence and uniqueness of the global extrema.

Table 3. Lifetimes of 72 cavia porcellus injected with different dosages of Mycobacterium tuberculosis.

Lifetimes (in days)					
12	44	60	70	95	146
15	48	60	72	96	175
22	52	60	73	98	175
24	53	60	75	99	211
24	54	61	76	109	233
32	54	62	76	110	258
32	55	63	81	121	258
33	56	65	83	127	263
34	57	65	84	129	297
38	58	67	85	131	341
38	58	68	87	143	341
43	59	70	91	146	376

*The **R** source code of this study is available from the author upon request.

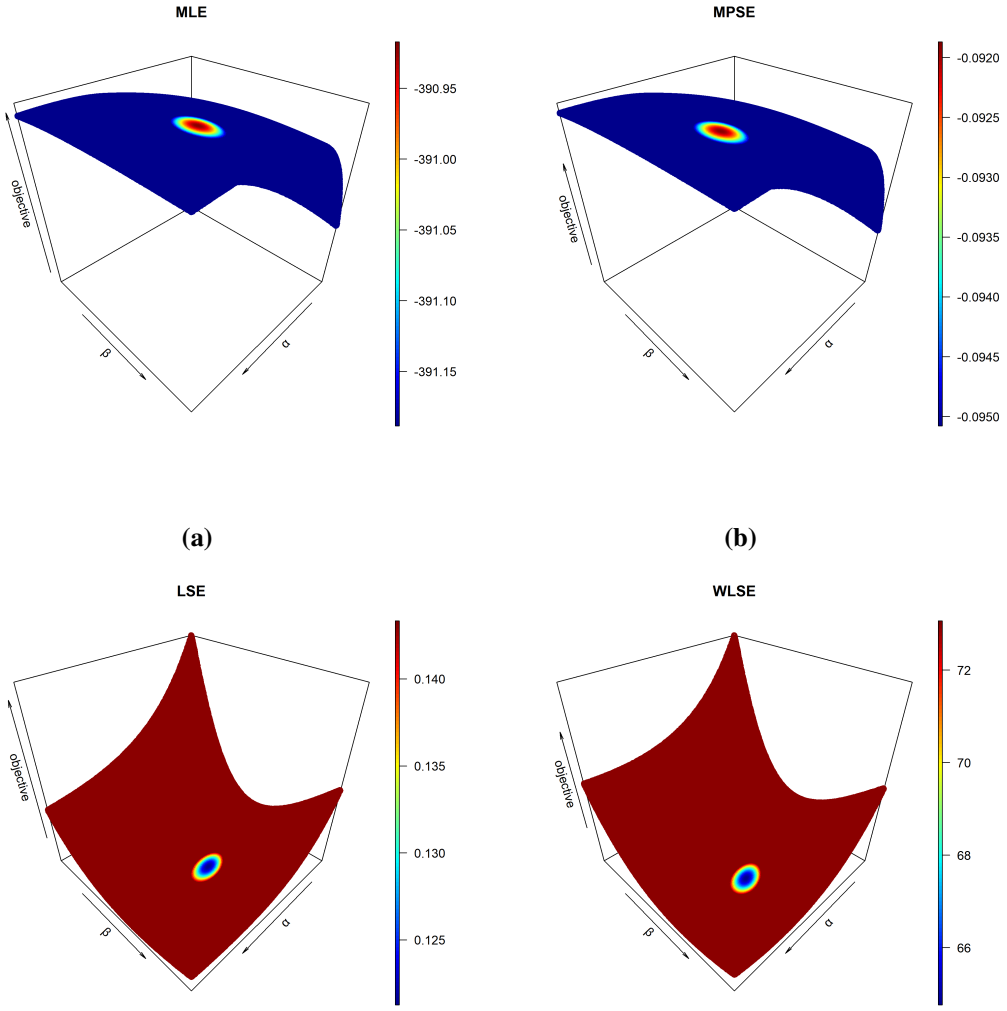

Figure 7. Three-dimensional surface plots of the objective functions for the nine estimation methods applied to the data in Table 3. The distinct peak in each plot demonstrates the presence of a unique optimum.

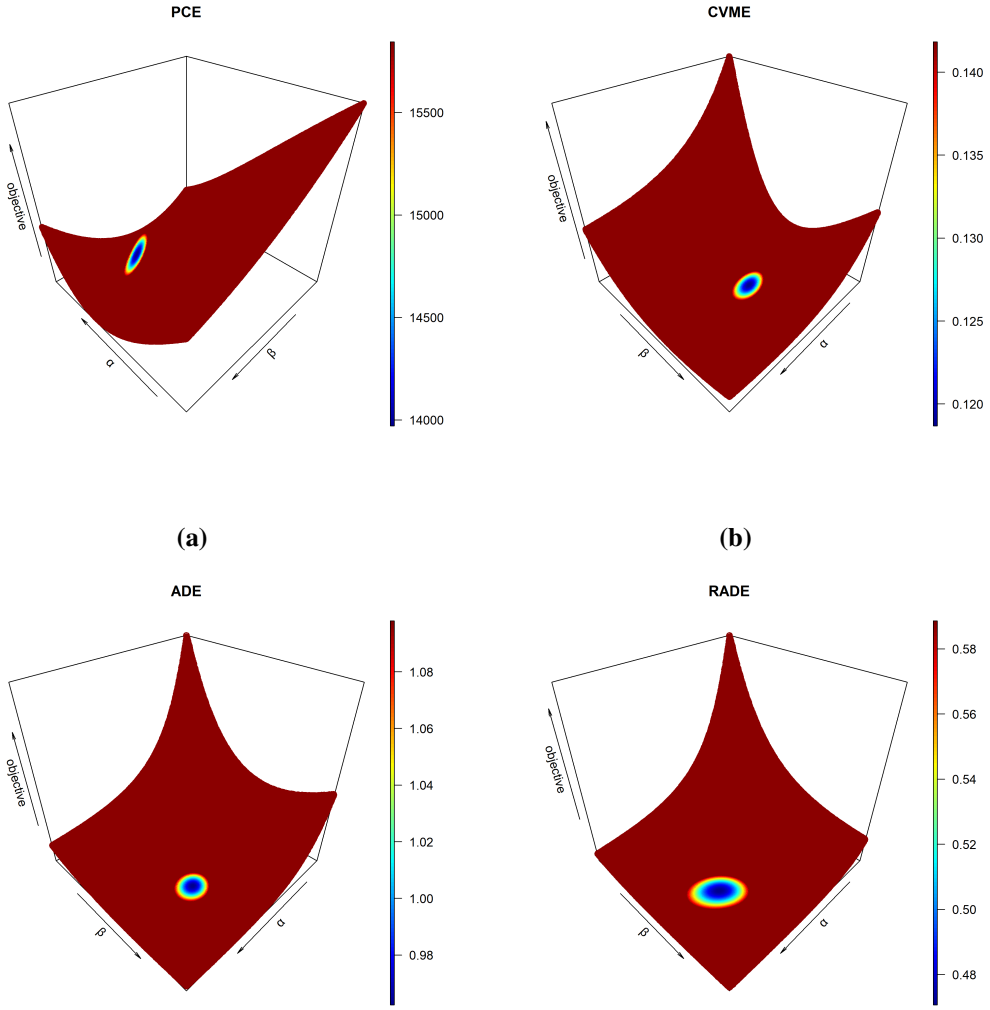

Figure 8. Three-dimensional surface plots of the objective functions for the nine estimation methods applied to the data in Table 3. The distinct peak in each plot demonstrates the presence of a unique optimum (cont.).

Table 4 reports the parameter estimates $(\hat{\alpha},\hat{\beta})$ obtained from the nine estimation methods considered, together with the corresponding goodness-of-fit results from the one-sample Kolmogorov-Smirnov (KS) test and the estimated change point $c_{\hat{\alpha},\hat{\beta}}$. Since ties exist in the dataset, the MPSEs cannot be directly obtained; however, a generalization of the maximum product of spacings method may be applied to address this issue (see [46] for details). The table summarizes results under three settings: (a) no data contamination, (b) 7% upper contamination by doubling the largest five observations, and (c) percentage errors arising from contamination. The latter table also includes percentage errors that are used to numerically assess the robustness of the competing estimators, as well as parametric bootstrap standard errors (SEs) computed using 1000 parametric bootstrap resamples for all nine estimation methods. These results provide additional insight into the sampling stability of the estimators.

Table 4. Fitted models and outcomes of goodness-of-fit: (a) no contamination; (b) 7% upper contamination; (c) percentage errors due to contamination.

Part (a)								
Method	$\hat{\alpha}$	SE$^*(\hat{\alpha})$	$\hat{\beta}$	SE$^*(\hat{\beta})$	$c_{\hat{\alpha},\hat{\beta}}$	SE$^*(c_{\hat{\alpha},\hat{\beta}})$	KS	p-value
MME	0.76	0.064	77.453	6.755	90.301	31.735	0.104	0.413
MLE	0.76	0.064	77.535	6.763	90.397	31.777	0.104	0.419
LSE	0.638	0.069	74.311	5.886	153.846	62.423	0.092	0.571
WLSE	0.692	0.066	75.764	6.297	119.598	45.458	0.098	0.497
PCE	0.889	0.201	72.678	10.821	52.339	27.957	0.158	0.055
MPSE	0.816	0.081	76.899	7.142	71.773	20.699	0.12	0.249
CVME	0.621	0.066	74.229	5.736	167.994	74.516	0.088	0.636
ADE	0.731	0.067	76.377	6.659	100.908	35.971	0.104	0.419
RADE	0.786	0.080	74.946	7.317	78.701	34.631	0.125	0.207
Part (b)								
Method	$\hat{\alpha}$	SE$^*(\hat{\alpha})$	$\hat{\beta}$	SE$^*(\hat{\beta})$	$c_{\hat{\alpha},\hat{\beta}}$	SE$^*(c_{\hat{\alpha},\hat{\beta}})$	KS	p-value
MME	0.918	0.077	86.011	8.812	56.329	18.575	0.161	0.047
MLE	0.919	0.077	87.145	8.928	57.048	18.821	0.167	0.036
LSE	0.633	0.069	74.244	5.840	157.442	63.759	0.091	0.584
WLSE	0.674	0.065	75.373	6.105	130.209	49.384	0.095	0.531
PCE	1.763	3.079	46.691	21.388	5.974	6.361	0.345	< 0.001
MPSE	0.988	0.098	87.199	9.493	46.375	12.532	0.171	0.03
CVME	0.617	0.065	74.178	5.701	171.058	75.706	0.087	0.646
ADE	0.811	0.075	77.848	7.478	73.868	25.701	0.114	0.308
RADE	0.943	0.097	75.235	8.739	45.729	19.173	0.152	0.071
Part (c)								
Method	$\hat{\alpha}$	SE$^*(\hat{\alpha})$	$\hat{\beta}$	SE$^*(\hat{\beta})$	$c_{\hat{\alpha},\hat{\beta}}$	SE$^*(c_{\hat{\alpha},\hat{\beta}})$	KS	p-value
MME	20.79%	20.95%	11.05%	30.47%	37.62%	41.47%	54.81%	88.62%
MLE	20.92%	20.98%	12.39%	32.02%	36.89%	40.77%	60.58%	91.41%
LSE	0.78%	0.72%	0.09%	0.79%	2.34%	2.14%	1.09%	2.28%
WLSE	2.60%	2.70%	0.52%	3.06%	8.87%	8.64%	3.06%	6.84%
PCE	98.31%	$> 100\%$	35.76%	97.66%	88.59%	77.25%	118.35%	100.00%
MPSE	21.08%	21.05%	13.39%	32.92%	35.39%	39.46%	42.50%	87.95%
CVME	0.64%	0.56%	0.07%	0.62%	1.82%	1.60%	1.14%	1.57%
ADE	10.94%	11.03%	1.93%	12.31%	26.80%	28.55%	9.62%	26.49%
RADE	19.97%	20.27%	0.39%	19.43%	41.90%	44.64%	21.60%	65.70%

Table 4 indicates that the robust methods were the LSE, WLSE, and CVME since the bootstrap SEs for the estimators of the model parameters and the change point were consistently small, and the associated percentage errors did not exceed 3%. This confirms that these methods are not only efficient, as seen in the simulation study, but also display high stability under repeated sampling. In contrast, the percentile estimator (PCE) exhibited extremely large bootstrap SEs, with percentage errors exceeding 70% for the change point and over 100% for the shape parameter α. This indicates a severe lack of robustness and highlights the sensitivity of percentile-based procedures to sampling variability in contaminated data. The remaining methods (MME, MLE, MPSE, ADE, and RADE) showed moderate to high bootstrap variability, with percentage errors ranging from 20% to 45%. Taken together, the bootstrap results reinforce the main conclusion of this study: among the nine estimators considered, LSE, WLSE, and CVME provide the most reliable balance of accuracy and robustness for change point estimation in the Birnbaum-Saunders model under contamination. To further support the conclusions, and under the same assumptions, Table 5 reports observed and fitted exploratory data analysis (EDA) results, including the sample mean, median, quartiles, standard deviation (SD), coefficient of skewness (CS), and coefficient of kurtosis (CK). Overall, CVMEs, LSEs, and WLSEs show satisfactory performance, as the percentage errors suggest that these methods are not substantially

affected by contamination.

Table 5. Outcomes of EDA: (a) no contamination; (b) 7% upper contamination; (c) percentage errors due to contamination.

Part (a)

Source	Q_1	Median	Mean	Q_3	SD	CS	CK
Sample	54.750	70.000	99.819	112.75	81.118	1.796	5.614
MME	46.643	77.453	99.819	128.613	77.241	2.077	6.845
MLE	46.692	77.535	99.925	128.750	77.323	2.077	6.845
LSE	48.489	74.311	89.424	113.884	58.209	1.803	5.217
WLSE	47.699	75.764	93.914	120.344	66.311	1.929	5.943
PCE	40.245	72.678	101.404	131.248	91.113	2.330	8.514
MPSE	44.654	76.899	102.491	132.430	84.915	2.192	7.578
CVME	48.977	74.229	88.539	112.502	56.109	1.762	4.994
ADE	46.877	76.377	96.781	124.442	72.100	2.015	6.460
RADE	44.387	74.946	98.068	126.543	78.352	2.13	7.182

Part (b)

Source	Q_1	Median	Mean	Q_3	SD	CS	CK
Sample	54.750	70.000	122.292	112.750	154.818	2.909	10.739
MME	46.734	86.011	122.292	158.299	113.237	2.383	8.878
MLE	47.346	87.145	123.915	160.401	114.755	2.383	8.880
LSE	48.592	74.244	89.128	113.439	57.599	1.792	5.156
WLSE	48.038	75.373	92.468	118.262	63.547	1.887	5.693
PCE	15.109	46.691	119.245	144.288	181.923	3.281	16.071
MPSE	45.300	87.199	129.794	167.855	128.451	2.500	9.717
CVME	49.056	74.178	88.317	112.165	55.653	1.754	4.948
ADE	45.333	77.848	103.480	133.685	85.298	2.183	7.522
RADE	40.248	75.235	108.661	140.636	103.035	2.425	9.173

Part (c)

Source	Q_1	Median	Mean	Q_3	SD	CS	CK
Sample	0.00%	0.00%	22.51%	0.00%	90.86%	61.97%	91.29%
MME	0.20%	11.05%	22.51%	23.08%	46.60%	14.73%	29.70%
MLE	1.40%	12.39%	24.01%	24.58%	48.41%	14.73%	29.73%
LSE	0.21%	0.09%	0.33%	0.39%	1.05%	0.61%	1.17%
WLSE	0.71%	0.52%	1.54%	1.73%	4.17%	2.18%	4.21%
PCE	62.46%	35.76%	17.59%	9.94%	99.67%	40.82%	88.76%
MPSE	1.45%	13.39%	26.64%	26.75%	51.27%	14.05%	28.23%
CVME	0.16%	0.07%	0.25%	0.30%	0.81%	0.45%	0.92%
ADE	3.29%	1.93%	6.92%	7.43%	18.31%	8.34%	16.44%
RADE	9.32%	0.39%	10.80%	11.14%	31.50%	13.85%	27.72%

For the practical interpretation of the results, consider the following discussion. In many practical applications, the hazard function is not monotone; rather, it increases up to a certain point and then decreases. For instance, in a study of breast cancer recovery, [31] reported that the mortality rate peaked about three years after diagnosis and subsequently declined gradually over a fixed period. Similarly, results from the Veteran Administration lung cancer trial showed inverted hazard patterns for both low- and high-performance status groups [47]. In such contexts, a key quantity of interest is the time at which the hazard function reaches its maximum [48]. Assuming uncontaminated data, Table 4 indicates that this maximum mortality is expected to occur at approximately 53 days according to the PCEs and 168 days according to the CVMEs.

5. Conclusions

The hazard rate is a fundamental statistical measure in reliability and survival analysis, and identifying its change point enables researchers to make informed interventions and reduce potential costs. This study extends previous work by comparing nine frequentist procedures for estimating the change point of the Birnbaum-Saunders hazard rate under contaminated data. Simulation results demonstrated that CVMEs, LSEs, and WLSEs achieved the most robust performance in terms of bias and RMSE, while MME, MLE, PCE, MPSE, ADE, and RADE were more sensitive to contamination, particularly for small sample sizes and shape parameters. The application to tuberculosis survival data further confirmed that CVME, LSE, and WLSE produced stable estimates even when the dataset was artificially contaminated. These findings suggest that in the presence of outliers, CVME-, LSE-, and WLSE-based approaches are preferable for change point estimation in BS models.

Several research directions remain open. Of particular importance is strengthening the theoretical basis of these estimation procedures, for example by studying the asymptotic properties of change point estimators and analyzing their robustness through influence functions. For instance. Other important directions include extending the methods to settings with missing or censored data and comparing the frequentist approaches considered here with Bayesian counterparts.

Acknowledgments

The author would like to express their sincere appreciation to the Editor and the anonymous reviewers for their valuable comments and constructive suggestions, which significantly improved the quality and clarity of this manuscript. Their time, effort, and insightful feedback are deeply appreciated. Moreover, this project was funded by KAU Endowment (WAQF) at King Abdulaziz University, Jeddah, Saudi Arabia. The author, therefore, acknowledges with thanks WAQF and the Deanship of Scientific Research (DSR) for technical and financial support.

This Project was funded by KAU Endowment (WAQF) at King Abdulaziz University, Jeddah, under grant The authors, therefore, acknowledge with thanks WAQF and the Deanship of Scientific Research (DSR) for technical and financial support

Use of Generative-AI tools declaration

The author declares that Generative Artificial Intelligence (AI) tools were used in the preparation of this article. In particular, ChatGPT-5 was employed to enhance the clarity, grammar, and readability of the text. All statistical analyses, numerical simulations, computations, derivations, tables, and figures were solely carried out by the author. Text refined with the assistance of AI appears throughout the introduction, methodology, and discussion sections; however, the scientific content and conclusions remain entirely the responsibility of the author.

Conflict of interest

The author declares no conflicts of interest in this paper.

References

1. D. Kundu, N. Kannan, N. Balakrishnan, On the hazard function of Birnbaum-Saunders distribution and associated inference, *Comput. Stat. Data Anal.*, **52** (2008), 2692–2702. https://doi.org/10.1016/j.csda.2007.09.021
2. M. Bebbington, C. D. Lai, R. Zitikis, A proof of the shape of the Birnbaum-Saunders hazard rate function, *Math. Sci.*, **33** (2008), 49–56.
3. C. Azevedo, V. Leiva, E. Athayde, N. Balakrishnan, Shape and change point analyses of the Birnbaum-Saunders-*t* hazard rate and associated estimation, *Comput. Stat. Data Anal.*, **56** (2012), 3887–3897. https://doi.org/10.1016/j.csda.2012.05.007
4. F. M. A. Alam, A. Mansour Almalki, The hazard rate function of the logistic Birnbaum-Saunders distribution: Behavior, associated inference, and application, *J. King Saud Univ. Sci.*, **33** (2021), 101580. https://doi.org/10.1016/j.jksus.2021.101580
5. R. D. Gupta, D. Kundu, Generalized exponential distribution: Different method of estimations, *J. Stat. Comput. Simul.*, **69** (2001), 315–337. https://doi.org/10.1080/00949650108812098
6. M. R. Alkasasbeh, M. Z. Raqab, Estimation of the generalized logistic distribution parameters: Comparative study, *Stat. Methodol.*, **6** (2009), 262–279. https://doi.org/10.1016/j.stamet.2008.10.001
7. J. Mazucheli, F. Louzada, M. E. Ghitany, Comparison of estimation methods for the parameters of the weighted Lindley distribution, *Appl. Math. Comput.*, **220** (2013), 463–471. https://doi.org/10.1016/j.amc.2013.05.082
8. A. P. J. do Espirito Santo, J. Mazucheli, Comparison of estimation methods for the Marshall-Olkin extended Lindley distribution, *J. Stat. Comput. Simul.*, **85** (2015), 3437–3450. https://doi.org/10.1080/00949655.2014.977904
9. F. M. A. Alam, F. Khalawi, A. M. Daghistani, Modeling fatigue data of complex metallic alloys using a generalized Student's t-Birnbaum-Saunders family of lifetime models: A comparative study with applications, *Crystals*, **15** (2025), 575. https://doi.org/10.3390/cryst15060575
10. C. Lawson, J. B. Keats, D. C, Montgomery. Comparison of robust and least-squares regression in computer-generated probability plots, *IEEE T. Reliab.*, **46** (1997), 108–115. https://doi.org/10.1109/24.589935
11. K. Boudt, D. Caliskan, C. Croux, Robust explicit estimators of Weibull parameters, *Metrika*, **73** (2011), 187–209. https://doi.org/10.1007/s00184-009-0272-1
12. C. Agostinelli, A. Marazzi, V. J. Yohai, Robust estimators of the generalized log-gamma distribution, *Technometrics*, **56** (2014), 92–101. https://doi.org/10.1080/00401706.2013.818578
13. M. Wang, C. Park, X. Sun, Simple robust parameter estimation for the Birnbaum-Saunders distribution, *J. Stat. Distrib. Appl.*, **2** (2015), 14. https://doi.org/10.1186/s40488-015-0038-4
14. N. Balakrishnan, D. Kundu, Birnbaum-Saunders distribution: A review of models, analysis, and applications, *Appl. Stoch. Model. Bus.*, **35** (2019), 4–49. https://doi.org/10.1002/asmb.2348
15. Z. W. Birnbaum, S. C. Saunders, A new family of life distributions, *J. Appl. Probab.*, **6** (1969), 319–327. https://doi.org/10.2307/3212003

16. Z. W. Birnbaum, S. C. Saunders, Estimation for a family of life distributions with applications to fatigue, *J. Appl. Probab.*, **6** (1969), 328–347. https://doi.org/10.2307/3212004

17. A. Desmond, Stochastic models of failure in random environments, *Can. J. Stat.*, **13** (1985), 171—183. https://doi.org/10.2307/3315148

18. J. A. Diáz-Garciá, V. Leiva-Sánchez, A new family of life distributions based on the elliptically contoured distributions, *J. Stat. Plan. Infer.*, **128** (2005), 445–457. https://doi.org/10.1016/j.jspi.2003.11.007

19. J. A. Diáz-Garciá, V. Leiva-Sánchez, Erratum to "A new family of life distributions based on the elliptically contoured distributions": [J. Statist. Plann. Inference, 128 (2), (2005) 445-457], *J. Stat. Plan. Infer.*, **137** (2007), 1512–1513. https://doi.org/10.1016/j.jspi.2006.06.040

20. H. K. T. Ng, D. Kundu, N. Balakrishnan, Modified moment estimation for the two-parameter Birnbaum-Saunders distribution, *Comput. Stat. Data Anal.*, **43** (2003), 283–298. https://doi.org/10.1016/S0167-9473(02)00254-2

21. H. K. T. Ng, D. Kundu, N. Balakrishnan, Point and interval estimation for the two-parameter Birnbaum-Saunders distribution based on Type-II censored samples, *Comput. Stat. Data Anal.*, **50** (2006), 3222–3242. https://doi.org/10.1016/j.csda.2005.06.002

22. D. Kundu, N. Balakrishnan, A. Jamalizadeh, Bivariate Birnbaum-Saunders distribution and associated inference, *J. Multivar. Anal.*, **101** (2010), 113–125. https://doi.org/10.1016/j.jmva.2009.05.005

23. D. Kundu, N. Balakrishnan, A. Jamalizadeh, Generalized multivariate Birnbaum-Saunders distributions and related inferential issues, *J. Multivar. Anal.*, **116** (2013), 230–244. https://doi.org/10.1016/j.jmva.2012.10.017

24. A. J. Lemonte, G. Martínez-Florez, G. Moreno-Arenas, Multivariate Birnbaum-Saunders distribution: Properties and associated inference, *J. Stat. Comput. Simul.*, **85** (2015), 374–392. https://doi.org/10.1080/00949655.2013.823964

25. R. G. Aykroyd, V. Leiva, C. Marchant, Multivariate Birnbaum-Saunders distributions: Modelling and applications, *Risks*, **6** (2018), 21. https://doi.org/10.3390/risks6010021

26. M. Bourguignon, L. L. Ho, F. H. Fernandes, Control charts for monitoring the median parameter of Birnbaum-Saunders distribution, *Qual. Reliab. Eng. Int.*, **36** (2020), 1333–1363. https://doi.org/10.1002/qre.2632

27. H. Hassani, M. Kalantari, M. R. Entezarian, A new five-parameter Birnbaum-Saunders distribution for modeling bicoid gene expression data, *Math. Biosci.*, **319** (2020), 108275. https://doi.org/10.1016/j.mbs.2019.108275

28. G. Kannan, P. Jeyadurga, S. Balamurali, Economic design of repetitive group sampling plan based on truncated life test under Birnbaum-Saunders distribution, *Commun. Stat. Simul. C.*, **51** (2022), 7334–7350. https://doi.org/10.1080/03610918.2020.1831538

29. Y. Liu, H. Wang, X. Ma, A novel random-effect Birnbaum-Saunders distribution for reliability assessment considering accelerated mechanism equivalence, *Qual. Technol. Quant. M.*, **22** (2025), 752–778. https://doi.org/10.1080/16843703.2024.2400434

30. O. M. Bdair, Inference for two-parameter Birnbaum-Saunders distribution based on Type-II censored data with application to the fatigue life of aluminum coupon cuts, *Mathematics*, **13** (2025), 590. https://doi.org/10.3390/math13040590

31. A. O. Langlands, S. J. Pocock, G. R. Kerr, S. M. Gore, Long-term survival of patients with breast cancer: A study of the curability of the disease, *Br. Med. J.*, **2** (1979), 1247–1251. https://doi.org/10.1136/bmj.2.6200.1247

32. N. L. Johnson, S. Kotz, N. Balakrishnan, *Continuous univariate distributions, Volume 2*, John Wiley & Sons, 1995.

33. X. Zhu, N. Balakrishnan, Birnbaum-Saunders distribution based on Laplace kernel and some properties and inferential issues, *Stat. Prob. Lett.*, **101** (2015), 1–10. https://doi.org/10.1016/j.spl.2015.02.007

34. M. Engelhardt, L. J. Bain, F. T. Wright, Inferences on the parameters of the Birnbaum-Saunders fatigue life distribution based on maximum likelihood estimation, *Technometrics*, **23** (1981), 251–256. https://doi.org/10.2307/1267788

35. N. Balakrishnan, X. Zhu, On the existence and uniqueness of the maximum likelihood estimates of the parameters of Birnbaum-Saunders distribution based on Type-I, Type-II and hybrid censored samples, *Statistics*, **48** (2014), 1013–1032. https://doi.org/10.1080/02331888.2013.800069

36. J. J. Swain, S. Venkatraman, J. R. Wilson, Least-squares estimation of distribution functions in johnson's translation system, *J. Stat. Comput. Simul.*, **29** (1988), 271–297. https://doi.org/10.1080/00949658808811068

37. B. C. Arnold, N. Balakrishnan, H. N. Nagaraja, *A first course in order statistics*, Society for Industrial and Applied Mathematics, 2008.

38. J. H. K. Kao, Computer methods for estimating Weibull parameters in reliability studies, *IRE T. Reliab. Qual. Contr.*, **PGRQC-13** (1958), 15–22. https://doi.org/10.1109/IRE-PGRQC.1958.5007164

39. J. H. K. Kao, A graphical estimation of mixed Weibull parameters in life-testing of electron tubes, *Technometrics*, **1** (1959), 389–407. https://doi.org/10.1080/00401706.1959.10489870

40. H. Al-Mofleh, A. Z. Afify, N. A. Ibrahim, A new extended two-parameter distribution: Properties, estimation methods, and applications in medicine and geology, *Mathematics*, **8** (2020), 1578. https://doi.org/10.3390/math8091578

41. R. C. H. Cheng, N. A. K. Amin, Maximum product-of-spacings estimation with applications to the lognormal distribution, 1979.

42. R. C. H. Cheng, N. A. K. Amin, Estimating parameters in continuous univariate distributions with a shifted origin, *J. R. Stat. Soc. B*, **45** (1983), 394–403. https://doi.org/10.1111/j.2517-6161.1983.tb01268.x

43. B. Ranneby, The maximum spacing method. An estimation method related to the maximum likelihood method, *Scand. J. Stat.*, **11** (1984), 93–112.

44. K. Ghosh, S. R. Jammalamadaka, A general estimation method using spacings, *J. Stat. Plan. Infer.*, **93** (2001), 71–82. https://doi.org/10.1016/S0378-3758(00)00160-9

45. R Core Team, *R: A Language and Environment for Statistical Computing*, R Foundation for Statistical Computing, Vienna, Austria, 2016.

46. P. Murage, J. Mungátu, E. Odero, Optimal threshold determination for the maximum product of spacing methodology with ties for extreme events, *Open J. Model. Simul.*, **7** (2019), 149–168. https://doi.org/10.4236/ojmsi.2019.73008

47. S. Bennett, Log-logistic regression models for survival data, *Appl. Statist.*, **32** (1983), 165–171. https://doi.org/10.2307/2347295

48. R. C. Gupta, N. Kannan, A. Raychaudhuri, Analysis of lognormal survival data, *Math. Biosci.*, **139** (1997), 103–115. https://doi.org/10.1016/s0025-5564(96)00133-2

AIMS Press